Highly Stereoselective Formation of Cp*IrCl Complexes of *N*,*N*-Dimethylamino Acids

Douglas B. Grotjahn* and Camil Joubran

Department of Chemistry and Biochemistry, Box 871604, Arizona State University, Tempe, Arizona 85287-1604

John L. Hubbard†

Department of Chemistry and Biochemistry, Utah State University, Logan, Utah 84322-0300

Received October 5, 1995⊗

N,*N*-Dimethylamino acids serve as (N, O)-chelating monoanionic ligands to the prochiral fragment Cp*IrCl. A series of four such complexes and one Rh analog all were formed with diastereoselectivity of ≥50:≤1. The structure of the valine complex **5d** ($C_{17}H_{29}ClIrNO_2$) was analyzed at 298 K, from which a cis-arrangement of Cp* and valine side chain (*i*-Pr) was revealed. Solution NMR studies of **5d**, aided by an unusual zero coupling between the two methine protons of the amino acid, showed that the structures in solution and the solid were very similar. The preference for the cis-oriented Cp* and amino acid side chain in **5** is attributed to a maximum number of gauche interactions in the metallacycle and its substituents, especially pronounced for N,N-disubstituted amino acids.

Introduction

Amino acid−metal coordination complexes[1] are of interest in biochemistry.[2] Amino acids are sources of chiral, enantiomerically pure organometallic catalysts.[3] Some studies of organometallic amino acid complexes have focused on the bonding of fragments to the amino acid[4] (usually as a chelate, but see ref 5), whereas others have explored the asymmetric induction of the amino acid on coordination of a prochiral metal fragment.[6] For example, interaction of amino acid salts **1** with [Cp*IrCl-(μ-Cl)]$_2$ (**2**)[7] leads to **3** (Scheme 1), with essentially no diastereomeric excess in the case of N-unsubstituted amino acids and up to 84% de in the case of proline, an N-monosubstituted acid.[6a,b] We wanted to expand our investigations of the interactions of amino acids and transition metals[8] to include complexes similar to **3**. However, we initiated studies of the corresponding *N*,*N*-dimethyl amino acids **4** (Scheme 2), with the idea that the complexes would enjoy greater solubility in nonpolar organic solvents, the methyl groups would be convenient for monitoring reactions of **4** by NMR spectroscopy, and potential proton transfer involving metal-complexed NH_2 moieties[9] would be blocked. Here we report on the completely stereoselective (≥50:1) conversion of **4** to **5** and through X-ray crystallography and NMR spectros-

Scheme 1

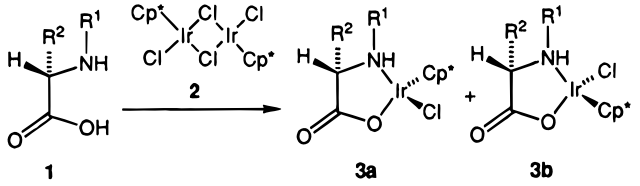

† X-ray crystal structure.

⊗ Abstract published in *Advance ACS Abstracts,* January 15, 1996.

(1) (a) Laurie, S. H. Amino Acids, Peptides and Proteins. In *Comprehensive Coordination Chemistry*; Wilkinson, G., Ed.; Pergamon: Oxford, 1987, Vol. 2, pp 739−776. (b) Ioganson, A. A. *Russ. Chem. Rev.* **1985**, *54*, 277−292. (c) Sigel, H.; Martin, R. B. *Chem. Rev.* **1982**, *82*, 385−426.

(2) Metalloproteins: Structural Aspects. *Adv. Prot. Chem.* **1991**, *42*. Ibers, J. A.; Holm, R. H. *Science* **1980**, *209*, 223−235. For a leading reference to organometallic complexes of other biomolecules, see: Chen, H.; Maestre, M.; Fish, R. H. *J. Am. Chem. Soc.* **1995**, *117*, 3631−3632.

(3) (a) Brunner, H. *Top. Stereochem.* **1988**, *18*, 129−247. (b) *Chiral Catalysis; Asymmetric Synthesis, Vol. 5*; Academic: Orlando, FL, 1984. (c) *Asymmetric Catalysis in Organic Synthesis*; Noyori, R., Ed.; Wiley: New York, 1994. (d) *Catalysis in Asymmetric Synthesis*; Ojima, I., Ed.; VCH: New York, 1993.

(4) (a) Dowerah, D.; Singh, M. M. *J. Ind. Chem. Soc.* **1980**, *57*, 368−371. (b) Dowerah, D.; Singh, M. M. *J. Chem. Res.* (S) **1979**, 38. (c) Dowerah, D.; Singh, M. M. *Transition Met. Chem.* **1976**, *1*, 294−5. (d) Shinoda, S.; Inoue, N.; Takita, K.; Saito, Y. *Inorg. Chim. Acta* **1982**, *65*, L21-L23. (e) Sheldrick, W. S.; Heeb, S. *J. Organomet. Chem.* **1989**, *377*, 357−366. (f) Sheldrick, W. S.; Exner, R. *Inorg. Chim Acta* **1990**, *175*, 261−268. (g) Lippmann, E.; Krämer, R.; Beck, W. *J. Organomet. Chem.* **1994**, *466*, 167−174. (h) Bergs, R.; Sünkel, K.; Beck, W. *Chem. Ber.* **1993**, *126*, 2429−2432. (i) Darensbourg, D. J.; Atnip, E. V.; Klausmeyer, K. K.; Reibenspies, J. H. *Inorg. Chem.* **1994**, *33*, 5230−5237. (j) Severin, K.; Sünkel, K.; Beck, W. *Chem. Ber.* **1994**, *127*, 615−620.

(5) Cp_2Ti(amino acid)$_2$ complexes: Klapötke, T. M.; Köpf, H.; Tornieporth-Oetting, I. C.; White, P. S. *Angew. Chem., Int. Ed. Engl.* **1994**, *33*, 1518−1519. Klapötke, T. M.; Köpf, H.; Tornieporth-Oetting, I. C.; White, P. S. *Organometallics* **1994**, *13*, 3628−3633. Tornieporth-Oetting, I. C.; White, P. S. *Organometallics* **1995**, *14*, 1632−1636.

(6) (a) Krämer, R.; Polborn, K.; Wanjek, H.; Zahn, I.; Beck, W. *Chem. Ber.* **1990**, *123*, 767−778. (b) Carmona, D.; Mendoza, A.; Lahoz, F. J.; Oro, L. A.; Lamata, M. P.; San Jose, E. *J. Organom. Chem.* **1990**, *396*, C17−C21. (c) Dersnah, D. F.; Baird, M. C. *J. Organomet. Chem.* **1977**, *127*, C55−C58. (d) Krämer, R.; Polborn, K.; Robl, C.; Beck, W. *Inorg. Chim. Acta* **1992**, *198*−200, 415−420. (e) Carmona, D.; Lahoz, F. J.; Atencio, R.; Oro. L. A.; Lamata, M. P.; San José, E. *Tetrahedron: Asymmetry* **1993**, 1425−1428. (f) Sheldrick, W. S.; Hauck, E.; Korn, S. *J. Organomet. Chem.* **1994**, *467*, 283−292. (g) Sheldrick, W. S.; Brandt, K. *Inorg. Chim. Acta* **1994**, *217*, 51−59. (h) Werner, H.; Daniel, T.; Nürnberg, O.; Knaup, W.; Meyer, U. *J. Organomet. Chem.* **1993**, *445*, 229−235. (i) Sheldrick, W. S.; Gleichmann, A. *J. Organomet. Chem.* **1994**, *470*, 183−187. (j) Sheldrick, W. S.; Exner, R. *Inorg. Chim. Acta* **1989**, *166*, 213−219.

(7) White, C.; Yates, A.; Maitlis, P. M. *Inorg. Synth.* **1992**, *29*, 228−234.

(8) Grotjahn, D. B.; Groy, T. L. *J. Am. Chem. Soc.* **1994**, *116*, 6969−6970; *Organometallics* **1995**, *14*, 3669−3682.

(9) Casalnuovo, A. L.; Calabrese, J. C.; Milstein, D. *Inorg. Chem.* **1987**, *26*, 971−973. Reviews: Bryndza, H. E.; Tam, W. *Chem. Rev.* **1988**, *88*, 1163−1188. Fryzuk, M. D.; Montgomery, C. D. *Coord. Chem. Rev.* **1989**, *95*, 1−40.

0276-7333/96/2315-1230$12.00/0

Table 1. Isolated Yield, Color, IR Data, and Elemental Analyses of 5

						calcd (%)			found (%)		
compd	R	yield (%)	color	IR ν_{CO} (cm^{-1})[a]	molecular formula	C	H	N	C	H	N
5a	CH_3	98	yellow	1652	$C_{15}H_{25}ClIrNO_2$	37.61	5.26	2.92	37.83	5.22	2.90
5b	Ph	96	yellow	1661	$C_{20}H_{27}ClIrNO_2$	44.39	5.03	2.59	44.56	5.12	2.53
5b′	Ph (Rh)	99	orange	1648	$C_{20}H_{27}ClRhNO_2$	53.17	6.02	3.10	52.84	6.04	3.16
5c	$PhCH_2$	81[b]	yellow		$C_{21}H_{29}ClIrNO_2$	45.44	5.27	2.52	45.48	5.31	2.46
5d	*i*-Pr	96	yellow	1656	$C_{17}H_{29}ClIrNO_2$	42.84	5.47	2.17	42.58	5.48	1.97

[a] In KBr. [b] Yield of recrystallized product from CH_2Cl_2−Et_2O. The crude yield was 100%.

Scheme 2

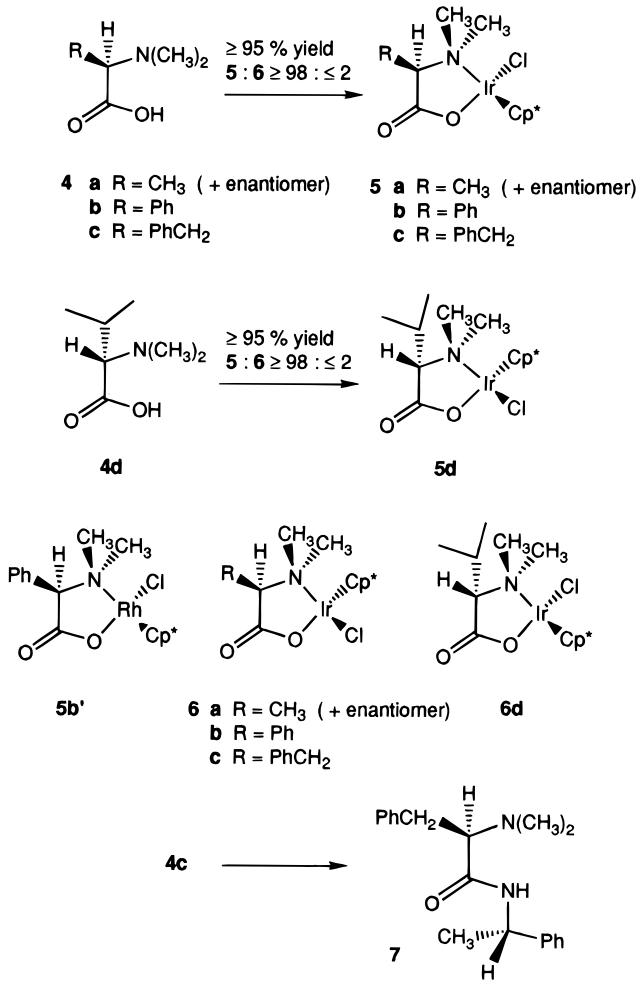

copy provide some insight into the origins of the high selectivity for **5**.

Results

Formation and Structure of 5 in the Solid and in Solution. The requisite *N*,*N*-dimethylamino acids **4** were made from **1** by known reductive amination methods.[10] Enantiomeric purity of **4b** was confirmed by DCC/HOBT-mediated coupling with (*S*)-α-methylbenzylamine, leading to **7** (88%),[11] none of the diastereomer being detected in the crude mixture.

Stirring **4**, **2**, and anhydrous K_2CO_3 (molar ratio 1.00:0.50:1.00) in acetonitrile for 12−36 h, followed by rotary evaporation, addition of CH_2Cl_2, filtration of the resulting mixture, and concentration, generally left **5** as analytically pure yellow or yellow-orange solid in ≥95% yields (see Table 1). The Rh analog of **2** was used to make **5b′**, an orange solid. Chelation of the amino acid to the metal was immediately evidenced by the appearance of two three-proton singlets in ^{1}H NMR spectra of **5**, ascribed to diastereotopic methyl protons; if the amino acid nitrogen were not bound to the metal, rapid inversion at N would lead to observation of a six-proton singlet for the methyl groups. Further, both ^{1}H and ^{13}C NMR spectral data for **5** (Tables 2 and 3) revealed the presence of resonances attributable to a *single* complex, whereas on the basis of literature precedent[6a,b] two were expected. From cursory inspection of NMR data and molecular models it was unclear which diastereomer should predominate, and the assumption that **5** had the same relative configuration as the major diastereomer **3a** previously observed seemed unwarranted.

Thus, single crystals of the valine derivative **5d** were grown by vapor diffusion of hexane into a toluene solution of the complex. The results of X-ray diffraction of **5d** are presented in Figure 1 and Tables 4−6. The molecular structure in Figure 1 verifies the composition of the product and the chelation of the amino acid. The absolute configuration of the complex is confirmed by refinement of the η parameter to a value of +1.1(1).[12] The geometry about the metal can be described as that of a three-legged piano stool,[13] with the two angles Cl−Ir−O(1) and Cl−Ir−N [88.1(3) and 87.7(3)°, respectively] being just under the ideal value of 90 and the N−Ir−O(1) angle being even more acute [76.4(4)°]. Very similar values for these and other metrical parameters were observed in proline-derived complexes **3**.[6a,b] The greatest metrical difference between reported structures of **3** and that of **5a** appears to be that the Ir−N distance in **5d** [2.158(11) Å] is slightly larger than the highest value reported for **3** [2.140(8) Å].[6b] This could be a result of the greater bulk of *N*,*N*-dimethyl substituents at N compared to the single *N*-alkyl group in proline.

Whereas **3** was obtained as a mixture of diastereomers **3a** and **3b**, **5d** is formed as a single diastereomer, with the largest metallacycle substituents, *i*-Pr and Cp*, cis to each other, as in **3a**. Both the *i*-Pr and Cp* groups occupy pseudoequatorial positions. Insight into the conformational and sterochemical preference for the systems **3** and **5** is gained by examining the relative orientations of the metallacycle substituents. The C(8)−C(7) bond to the $CH(CH_3)_2$ group is gauche to both of the N−CH_3 bonds, as indicated by torsional angles C(8)−C(7)−N−C(12) = +65.9° and C(8)−C(7)−N−C(11) = −54.2°, respectively. Similarly, the vector from Ir to the centroid of the Cp* ring (C*) is gauche to both the N−CH_3 bonds, as revealed by the torsional angles C*−Ir−N−C12 = −72.3° and C*−Ir−N−C11 = 49.6°,

(10) Bowman, R. E.; Staoud, H. H. *J. Chem. Soc.* **1950**, 1342−1345.
(11) The enantiomer has been reported: Takeuchi, S.; Ohgo, Y. *Bull. Chem. Soc. Jpn.* **1981**, *54*, 2136−2141.
(12) Rogers, D. *Acta Crystallogr., Sect. A* **1981**, *A37*, 734−741.
(13) Isobe, K.; Bailey, P. M.; Maitlis, P. M. *J. Chem. Soc., Dalton Trans.* **1981**, 2003−2008.

Table 2. ^{1}H NMR (δ, ppm) Data for 5[a]

compd	solvent	$C_5(CH_3)_5$	$N(CH_3)_2$	CHR	R
5a	$CDCl_3$	1.55 (s, 15H)	2.92 (s, 3H) 2.93 (s, 3H)	4.18 (q, J = 6.8, 1H)	1.08 (d, J = 6.8, 3H)
	CD_3CN	1.54 (s, 15H)	2.91 (s, 3H) 2.92 (s, 3H)	3.97 (q, J = 7.2, 1H)	1.02 (d, J = 7.2, 3H)
	C_6D_6	1.08 (s, 15H)	2.28 (s, 3H) 2.46 (s, 3H)	4.44 (q, J = 7.0, 1H)	0.96 (d, J = 7.0, 3H)
5b	$CDCl_3$	1.59 (s, 15H)	2.84 (s, 3H) 2.85 (s, 3H)	5.29 (s, 1H)	7.2−7.33 (m, 5H)
	CD_3CN	1.57 (s, 15H)	2.815 (s, 3H) 2.841 (s, 3H)	5.05 (s, 1H)	7.19−7.26 (m, 2H) 7.32−7.42 (m, 3H)
5b′	$CDCl_3$	1.60 (s, 15H)	2.66 (s, 3H) 2.67 (s, 3H)	4.96 (s, 1H)	7.12−7.21 (m, 2H) 7.21−7.30 (m, 3H)
	CD_3CN	1.60 (s, 15H)	2.663 (s, 3H) 2.669 (s, 3H)	4.75 (s, 1H)	7.14−7.20 (m, 2H) 7.29−7.37 (m, 3H)
5c	$CDCl_3$	1.53 (s, 15H)	2.76 (s, 3H) 3.10 (s, 3H)	4.57 (dd, J = 5.3, 7.9, 1H)	2.75 (dd, J = 7.9, 15.4, 1H) 3.39 (dd, J = 5.3, 15.4, 1H) 7.08−7.17 (m, 1H) 7.18−7.28 (m, 4H)
	CD_3CN	1.53 (s, 15H)	2.97 (s, 3H) 3.04 (s, 3H)	4.23 (dd, J = 3.7, 8.0, 1H)	2.81 (dd, J = 3.7, 14.2, 1H) 2.93 (dd, J = 8.0, 14.2, 1H) 7.13−7.21 (m, 1H) 7.23−7.30 (m, 4H)
5d	$CDCl_3$	1.54 (s, 15H)	3.00 (s, 3H) 3.07 (s, 3H)	3.84 (s, 1H)	1.12 (d, J = 6.7, 3H) 1.15 (d, J = 7.2, 3H) 1.96 (septet, J = 7, 1H)
	CD_3CN	1.53 (s, 15H)	2.98 (s, 3H) 3.07 (s, 3H)	3.65 (s, 1H)	1.06 (d, J = 6.7, 3H) 1.09 (d, J = 7.4, 3H) 1.93 (septet, J = 7, 1H)

[a] Multiplicity and coupling constants (Hz) in parentheses. Values referenced to residual $CHCl_3$ (7.24), CHD_2CN (1.93), or C_6HD_5 (7.15 ppm). Spectra were measured at ambient probe temperature at 300 MHz.

Table 3. ^{13}C NMR (δ, ppm) Data for 5[a]

compd	solvent	$C_5(CH_3)_5$	$C_5(CH_3)_5$	$N(CH_3)_2$	CHR	CO_2	R
5a	$CDCl_3$	84.35	8.62	48.97 49.18	65.89	182.58	*b*
	CD_3CN	85.61	9.09	49.92 50.16	67.13	182.95	9.52
5b	$CDCl_3$[c]	84.48	8.68	49.23 50.73	74.82	179.75	127.99 128.83 130.48 133.53
	CD_3CN	85.85	9.16	50.40 51.90	76.22	180.52	129.02 129.94 132.92 134.91
5b′	$CDCl_3$	93.20 (d, J = 8.5)	8.71	47.79 48.20	75.47	176.81	127.82 128.55 130.62 133.33
	CD_3CN	94.68 (d, J = 9.2)	9.21	48.88 49.26	76.89	177.55	128.07 129.66 133.07 134.70
5c	$CDCl_3$	84.28	8.62	49.59 50.50	71.52	181.20	31.76 139.82 126.41 128.78 128.98
	CD_3CN	85.72	9.09	50.17 50.47	73.20	182.02	31.41 142.07 127.42 129.78 130.60
5d	$CDCl_3$	84.20	8.90	49.69 51.63	73.92	179.40	19.22 23.37 23.75
	CD_3CN	85.52	9.07	50.38 52.46	75.31	180.82	19.42 23.86 24.29

[a] Singlets unless otherwise specified; coupling constants in Hz. Values referenced to $CDCl_3$ at 77.00 ppm or CD_3CN at 1.30 ppm. Spectra were measured at ambient probe temperature at 75.5 MHz. [b] Not seen. May be isochronous with $C_5(CH_3)_5$ resonance. [c] $CDCl_3$ data measured on racemic sample.

respectively. Finally, in **5d** the chloride ligand avoids eclipsing either N−CH_3 bond: the C(11) methyl is trans to Cl, whereas the cis C(12) methyl is gauche to Cl [torsional angle Cl−Ir−N−C(12) = 65.0°]. Our working

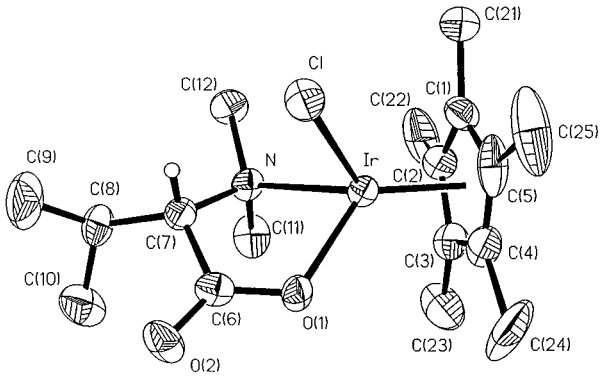

Figure 1. Molecular structure of **5d**, shown with 30% thermal ellipsoids. Hydrogen atoms other than that shown (assumed position of H(7a)) are omitted for clarity.

Table 4. Crystallographic Data for 5d

empirical formula	$C_{17}H_{29}NO_2ClIr$
color; habit	yellow blocks
cryst size (mm)	0.4 × 0.5 × 0.6
cryst system	orthorhombic
space group	$P2_12_12_1$
cell consts (Å)	$a = 10.905(2)$
	$b = 12.820(2)$
	$c = 13.751(2)$
V (Å^3)	1922.4(4)
Z	4
fw	507.1
D(calcd) (g/cm^3)	1.75
abs coeff (mm^{-1})	7.09
F(000)	992
diffractometer used	Siemens P4/Series II
radiation	Mo Kα ($\lambda = 0.710\ 73$ Å)
temp (K)	298
monochromator	highly oriented graphite cryst
2θ range (deg)	3−55
scan type	2θ−θ
scan speed	variable 3.00 to 15.00°/min in ω
scan range (ω)	1.20° plus Kα separation
bkgd measment	stationary cryst and stationary counter at beginning and end of scan, each for 25.0% of tot scan time
std reflcns	2 measd every 100 reflcns
index ranges	$0 \le h \le 14$; $0 \le k \le 16$; $0 \le l \le 17$
reflcns collcd	2551
indepdt reflcns	2530 ($R_{int} = 1.7\%$)
obsd reflcns	1973 ($F > 4\ \sigma$(F))
abs corr	empirical, ψ scan
min/max transm	0.75/1.0
soln and refinement	Siemens SHELXTLPLUS (VMS)
soln method	Patterson
refinement method	full-matrix least-squares
quant minimized	$\sum w(F_o - F_c)^2$
H atoms	riding model, fixed isotropic U
weighting scheme	$w^{-1} = \sigma^2(F) + 0.0012F^2$
no. of params	200
final R indices for obsd reflcns	$R = 0.0412$, w$R = 0.0467$
final R indices for indepdt reflcns	$R = 0.0774$, w$R = 0.0878$
goodness-of-fit	0.95
η-param	1.1(1)
largest and mean Δ/σ	0.001, 0.000
data-to-param ratio	9.9:1
largest diff peak (e/Å^3)	0.75

Table 5. Atomic Coordinates (×10^4) and Equivalent Isotropic Displacement Coefficients (Å^3 × 10^3)

	x	y	z	U_{eq}[a]
Ir	−1739(1)	−7793(1)	−8277(1)	42(1)
Cl	123(4)	−8588(3)	−8867(3)	65(1)
C(1)	−2433(15)	−7375(14)	−9682(11)	63(6)
C(2)	−2965(14)	−6723(12)	−8991(11)	58(5)
C(3)	−3630(12)	−7331(15)	−8308(13)	67(5)
C(4)	−3489(19)	−8420(17)	−8617(15)	80(7)
C(5)	−2786(19)	−8453(12)	−9445(17)	85(8)
C(21)	−1703(19)	−6997(19)	−10531(11)	98(9)
C(22)	−2984(22)	−5580(15)	−9039(16)	118(11)
C(23)	−4446(17)	−6919(25)	−7496(15)	131(13)
C(24)	−4054(19)	−9364(18)	−8103(22)	153(14)
C(25)	−2433(21)	−9357(17)	−10043(18)	147(12)
N	−606(10)	−6771(8)	−7410(8)	48(4)
O(1)	−1498(9)	−8614(6)	−6989(7)	51(3)
O(2)	−199(12)	−8937(7)	−5781(7)	70(4)
C(6)	−538(14)	−8419(10)	−6470(10)	53(5)
C(7)	208(12)	−7454(10)	−6791(10)	50(4)
C(8)	968(14)	−6912(13)	−6005(12)	64(6)
C(9)	2210(19)	−7430(20)	−5934(17)	117(11)
C(10)	398(22)	−6813(15)	−5005(11)	98(8)
C(11)	−1420(15)	−6142(12)	−6760(13)	71(6)
C(12)	156(17)	−6072(13)	−8004(12)	77(6)

[a] $U_{eq} = {}^1/_3\sum_i\sum_j U_{ij}a_i^*a_j^*a_ia_j$.

Table 6. Bond Lengths (Å) and Selected Angles (deg) for 5d

Ir−Cl	2.413(4)	C(3)−C(23)	1.521(27)
Ir−C(1)	2.144(15)	C(4)−C(5)	1.374(31)
Ir−C(2)	2.153(15)	C(4)−C(24)	1.531(32)
Ir−C(3)	2.146(14)	C(5)−C(25)	1.471(30)
Ir−C(4)	2.123(20)	N−C(7)	1.510(17)
Ir−C(5)	2.145(22)	N−C(11)	1.496(20)
Ir−N	2.158(11)	N−C(12)	1.471(20)
Ir−O(1)	2.076(9)	O(1)−C(6)	1.293(18)
C(1)−C(2)	1.392(22)	O(2)−C(6)	1.214(17)
C(1)−C(5)	1.472(25)	C(6)−C(7)	1.544(19)
C(1)−C(21)	1.494(24)	C(7)−C(8)	1.530(21)
C(2)−C(3)	1.420(23)	C(8)−C(9)	1.511(26)
C(2)−C(22)	1.467(24)	C(8)−C(10)	1.515(24)
C(3)−C(4)	1.468(28)		
Cl−Ir−N	87.7(3)	C(4)−C(5)−C(25)	129.3(18)
Cl−Ir−O(1)	88.1(3)	Ir−N−C(7)	107.2(7)
N−Ir−O(1)	76.4(4)	Ir−N−C(11)	108.5(9)
C(2)−C(1)−C(5)	107.7(15)	C(7)−N−C(11)	108.9(11)
C(2)−C(1)−C(21)	124.1(17)	Ir−N−C(12)	112.8(9)
C(5)−C(1)−C(21)	128.1(17)	C(7)−N−C(12)	109.5(11)
C(1)−C(2)−C(3)	109.6(14)	C(11)−N−C(12)	109.8(11)
C(1)−C(2)−C(22)	125.1(16)	Ir−O(1)−C(6)	118.4(8)
C(3)−C(2)−C(22)	124.8(16)	O(1)−C(6)−O(2)	124.8(13)
C(2)−C(3)−C(4)	106.0(15)	O(1)−C(6)−C(7)	115.1(11)
C(2)−C(3)−C(23)	126.5(18)	O(20)−C(6)−C(7)	120.1(13)
C(4)−C(3)−C(23)	127.1(18)	N−C(7)−C(6)	108.4(11)
C(3)−C(4)−C(5)	109.2(17)	N−C(7)−C(8)	117.0(11)
C(3)−C(4)−C(24)	125.2(18)	C(6)−C(7)−C(8)	116..6(12)
C(5)−C(4)−C(24)	125.6(19)	C(7)−C(8)−C(9)	109.3(14)
C(1)−C(5)−C(4)	107.5(16)	C(7)−C(8)−C(10)	117.2(14)
C(1)−C(5)−C(25)	123.2(19)	C(9)−C(8)−C(10)	110.3(16)

hypothesis is that the presence of *both N*-alkyl groups is responsible for the highly selective formation of **5** rather than **6**. For example, inspection of molecular models built on the basis of Figure 1a suggests that inversion at Ir by exchange of Cp* and Cl ligands (**6d**), without moving the other atoms of the complex, would place the Cp* and Cl ligands in eclipsing positions to the N−CH_3 bonds. It appears that conformational changes in **6d** would not allow the Cl and Cp* substituents to achieve gauche orientation to the N−CH_3 bonds without engendering eclipsing interactions between the N−CH_3 bonds and the C(8)−C(7) and C(7)−H(7a) bonds.

The relationship of solid-state and solution structures was probed using **5d**, particularly because in ^{1}H NMR spectra of **5d** a surprising lack of observable three-bond coupling between the two methine protons was noted (Table 2). Using assumed positions for the hydrogen atoms in **5d**, the torsional angle H(7a)−C(7)−C(8)−

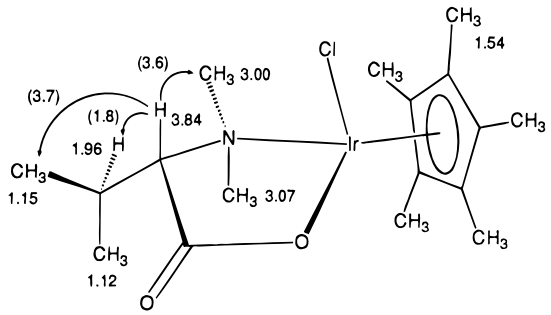

Figure 2. Proposed solution structure of **5d**. Chemical shifts (δ, ppm) are shown next to protons. nOe enhancements (in parentheses) are in percent.

H(8a) was determined to be 87.6°, explaining the absence of H−H coupling.[14] A series of nOe measurements[15] showing surprisingly specific enhancements also strongly suggested a solution conformation very close to that in Figure 1, depicted as Figure 2. Irradiation of the metallacycle methine H(7a) (84% saturation) led to enhancement of the upfield *N*-methyl singlet (3.6%), the *i*-Pr methine (1.8%), and the downfield *i*-Pr methyl group (3.7%). These data suggested the assignments shown in Figure 2. As in the remainder of this discussion, enhancements which amounted to less than 0.3% per H are regarded as insignificant. Conversely, irradiation of the upfield *N*-methyl singlet (δ 3.00 ppm) produced enhancements of the resonances for the methine protons H(7a) and H(8a) but almost no change in the *i*-Pr methyl signals and a slight enhancement of the singlet for the Cp* protons. Significantly, saturation of the the downfield N-methyl singlet (δ 3.07 ppm) led to 6% enhancement of the upfield *i*-Pr doublet, identified as the C(10) methyl, virtually no enhancement of the downfield *i*-Pr doublet, and significant enhancements of the H(8a) and Cp* singlets. Taken together, these data clearly identify the resonances at δ 3.07 and 3.00 as belonging to the C(11) and C(12) methyl protons, respectively. Remarkably, saturation of the Cp* singlet led to a greater enhancement of the singlet at δ 3.07 than of the singlet at 3.00 (4.1 vs 2.6%, respectively), consistent with the crystallographically determined C*−C(11) and C*−C(12) distances of 4.07 and 4.29 Å, respectively (Figure 2).

The configuration of the other members of the series is assumed to be the same as that of **5d**, which corresponds to the major isomer **3a** formed from N-unsubstituted or -monosubstituted amino acids.[6a,b] Infrared absorptions for the carboxylato carbonyl of **5** are similar to those for **3** and fall in the general range for monodentate carboxylato ligands in general.[16]

Discussion

Although a growing number of amino acid complexes to prochiral metal fragments have been reported,[6,8] few have been formed as **5** with complete diastereoselectivity. An explanation of observed diastereoselectivities has not been offered, nor has the effect of varying substitution at the amino acid nitrogen been explored. Among Cp*IrCl and Cp*RhCl complexes,[6a,b] **5** is formed with uniquely high diastereoselectivity, apparently a result of *N*,*N*-dialkyl substitution, rather than the bulk of the amino acid side chain. A Cp*CoCl complex to a cyclic *N*-monoalkyl amino acid was reported to be formed as a single diastereomer, also with *cis*-oriented Cp* and amino acid side chain.[6i] The complete selectivity may be a result of shorter metal−ligand bond lengths. On the other hand, the diastereomer of a Cp*Ir(CCtBu) chelate complex with Cp* and side chain *trans* was reported to be more stable.[6e] Related (benzene)Os(PR_3) complexes bearing bulky phosphines were reported to give chelates with *trans*-disposed arene and amino acid side chain,[6h] perhaps because the phosphine is actually bulkier than the benzene ligand.

Nonetheless, it appears that a cis-arrangement of Cp* and amino acid side chain is strongly preferred when the amino acid nitrogen bears two alkyl substituents and the remaining ligand on Ir (here, chloride) is relatively small compared to Cp*. In our previous work,[8] similar preference was seen when smaller ligands were added to Cp*Ir−amino acid complexes. These design criteria should aid the development of stereoselective organometallic and organic reactions using amino acid−metal complexes.

Experimental Section

General Methods. Although the compounds synthesized in this work all appear to be air-stable, all reactions were performed under nitrogen using Schlenk or glovebox techniques. However, workup was normally conducted in air, and solvent removal was conducted using a rotary evaporator. Other general experimental conditions were detailed elsewhere.[8] Elemental analyses were performed at Arizona State or at Atlantic Microlabs, Norcross, GA.

Formation of Chelate Complexes 5. Representative Procedure, Exemplified by 5b. Solid **2** (106.6 mg, 0.1339 mmol), **4b** (48.4 mg, 0.270 mmol, 2.02 mol/mol of **2**), and K_2CO_3 (42.1 mg, 0.305 mmol, 2.28 mol/mol of **2**) were combined in a 50 mL round-bottomed flask with a stir bar. Acetonitrile (26 mL) was added, the flask was capped with a septum, and the resulting yellow cloudy mixture was deoxygenated by bubbling nitrogen through it for 5 min using a syringe needle. The mixture was stirred for 17 h before it was concentrated and the residue was taken up in CH_2Cl_2 (10 mL). The resulting mixture was filtered through Celite, and the filter cake was rinsed with several portions of CH_2Cl_2 (total, 50 mL), until the filtrate was colorless. The combined yellow filtrates were concentrated and the yellow oily residue was scratched with Et_2O (5 mL) to obtain a yellow powder and a nearly colorless supernatant, which was removed using a pipet. Storage of the yellow powder under vacuum left **5b** (138.7 mg, 96%), mp 225−230 °C (dec) (the melting point of **5** seemed to depend on previous temperature and rate of heating and was not used as an indication of purity).

Crystal Structure of 5d. A crystal of **5d** was selected and mounted vertically in a 0.5 mm X-ray capillary and centered on a Siemens P4 autodiffractometer controlled at 25 °C. A primitive orthorhombic cell was determined from 25 randomly selected peaks with 2θ values between 15 and 30°. Data were collected in the $2\theta-\theta$ mode. Reduction of the data revealed the space group $P2_12_12_1$. Solution and refinement of the structure utilized the SHELXTL Plus package of programs from Siemens on a Vaxstation 3100 computer. The absolute configuration of the molecule was determined by the successful refinement of the η parameter[12] as a free variable, leading to a value of +1.1(1) for the enantiomer shown in Figure 1.

(14) For example: Abraham, R. J.; Fisher, J.; Loftus, P. *Introduction to NMR Spectroscopy*; Wiley: Chichester, U.K., 1988; Chapter 3, pp 34−59.

(15) Neuhaus, D.; Williamson, M. *The Nuclear Overhauser Effect in Structural and Conformational Analyses*; VCH: New York, 1989; Chapter 7.

(16) Nakamoto, K. *Infrared and Raman Spectra of Inorganic and Coordination Compounds*, 4th ed.; Wiley: New York, 1986.

nOe Characterization of 5d. The experiments were performed at ambient probe temperature in $CDCl_3$ at 400 Hz. Significant enhancements (≥0.3% per H) are listed.

resonance	T_1 (s)	% sat.	enhancements (ppm, %)
3.84	1.4	84	3.00, 3.6; 1.96, 1.8; 1.15, 3.7
3.07	0.5	89	3.84, 0.6; 1.96, 6.0; 1.54, 8.7; 1.12, 6.0
3.00	0.5	89	3.84, 6.1; 1.96, 7.2; 1.54, 5.1
1.96	0.8	62	3.84, 1.1; 3.07, 2.6; 3.00, 3.5; 1.15 and 1.12, 4.9
1.54	1.7	82	3.07, 4.1; 3.00, 2.6
1.15, 1.12	0.01−0.04	59	3.84, 3.3; 3.07, 3.2; 3.00, 0.6; 1.96, 5.0

Acknowledgment. We thank the ASU VP for Research for partial support of this work and Johnson Matthey Aesar/Alfa for a loan of iridium salts. We are grateful to Dr. Ron Nieman, the NSF (Grants CHE-88-13109, MPE 2498, and BBS 88-04992), and ASU for vital NMR instrumentation and instruction. J.L.H. acknowledges the NSF (Grant CHE-90-02379) for partial funding of the diffractometer.

Supporting Information Available: Crystallographic information on **5d**, including tables on bond distances and angles, anisotropic thermal parameters, and H positional and thermal parameters (3 pages). This material is contained in many libraries on microfiche, immediately follows this article in the microfilm edition of this journal, can be ordered from the ACS, and can be downloaded from the Internet; see any current masthead page for ordering information and Internet access instructions.

OM9507890